Pergamon

Geochimica et Cosmochimica Acta, Vol. 62, No. 7, pp. 1107–1118, 1998

0016-7037/98 $19.00 + .00

PII S0016-7037(98)00042-8

Effects of Quaternary sea level cycles on strontium in seawater

HEATHER M. STOLL[1,*] and DANIEL P. SCHRAG[2]

[1]Department of Geosciences, Princeton University, Princeton, New Jersey 08544, USA
[2]Department of Earth and Planetary Sciences, Harvard University, Cambridge, Massachusetts 02138, USA

(*Received June* 19, 1997; *accepted in revised form December* 11, 1997)

Abstract—The effects of Quaternary sea level changes on the Sr budget of the ocean are investigated using coupled numerical models of the seawater Sr and Ca budgets. Glacial/interglacial sea level cycles influence the Sr concentration of seawater directly through the periodic exposure and weathering of aragonite on continental shelves and indirectly by modulating the location and extent of carbonate deposition in the ocean. As sea level recedes, brief pulses of Sr are added to the ocean from recrystallization of shelf aragonite; this flux at its maximum is nearly ten times larger than the combined riverine and hydrothermal influx. The large shelf recrystallization fluxes during glacial maxima produce rapid increases in the Sr/Ca ratio of seawater despite the long residence time of Sr in the ocean. Variations in the ratio of aragonitic vs. calcitic sedimentation also influence on the Sr content of seawater because the Sr partitioning coefficient is higher in aragonite; however, this effect is minor compared to shelf aragonite recrystallization. Based on a variety of sensitivity tests, the amplitude of Sr/Ca variations ranges from 1 to 3 % and is maximized by constant rates of total carbonate deposition, extensive aragonite recrystallization, and carbonate budgets which include dissolution of shelf carbonates. Such variation is sufficient to produce up to 1.5°C errors in paleotemperatures calculated from coral Sr/Ca ratios since the last glacial maximum.

1. INTRODUCTION

Minor element chemistries and radiogenic isotopic ratios of marine carbonates, together with the $\delta^{18}O$ and $\delta^{13}C$ ratios, are primary sources of paleoceanographic information. Strontium in particular has been widely exploited, both in terms of its isotopic composition, which has been used as a chronostratigraphic tool and indicator of continental weathering intensity (Capo and DePaolo, 1990; Hess et al., 1989; Hodell et al., 1989), and the Sr concentration of seawater, used to understand geochemical cycles (Graham et al., 1982). More recently, the Sr/Ca ratio of scleractinian corals has been used as a paleotemperature indicator (Beck et al., 1992; Guilderson et al., 1994). A widely held belief is that the long residence time of Sr in the ocean implies static behavior over the short time scales of glacial cycles, and only over millions of years are there significant changes in the Sr concentration of the ocean. However, the recycling of Sr in aragonite on continental shelves gives rise to large changes in the flux of Sr to seawater, creating the potential for changes in the Sr concentration of seawater over glacial sea level cycles (Stoll and Schrag, 1996; Schlanger, 1988).

Strontium is added to the ocean by rivers and hydrothermal exchange and removed from the ocean by carbonate deposition, both in the form of aragonite and calcite. Biogenic aragonite has a much larger Sr partitioning coefficient than calcite (0.7–1.1 vs. 0.16–0.18; Roselle, 1985; Schlanger, 1988; Hess and Bender, 1986). Aragonitic coral and Halimeda algae, the predominant carbonate producers in shelf environments, have particularly high Sr concentrations (Schlanger, 1988). In contrast, low-Sr calcite is predominant in deep sea sediments. Consequently, changes in the accumulation rate of shelf vs. deep sea carbonates in response to sea level changes can affect the Sr concentration of seawater (Graham et al., 1982; Turekian, 1963). More importantly, when Sr-rich aragonitic sediments on the shelf are subaerially exposed during sea level regressions, recrystallization of aragonite to calcite in meteoric water releases most of the Sr. A complication results from the fact that Sr incorporation into carbonate partitions as the Sr/Ca ratio, so synchronous changes in Ca fluxes may partially mask changes in Sr fluxes. However, because the recrystallization of aragonite to calcite conserves Ca, recycling of Sr from continental shelves can change the Sr/Ca ratio of seawater.

Variations in the ratio of shelf to deep sea sediments and recrystallization of exposed aragonite both lead to higher Sr/Ca ratios during sea level regressions. Large fluctuations in seawater Sr/Ca ratios recorded in pelagic sediments have been used to identify rapid sea level changes in the Cretaceous, when the effect was magnified by more extensive areas of shelf carbonate accumulation and a lower residence time of Sr in the ocean (Stoll and Schrag, 1996). Because aragonite recrystallization is both extensive and rapid (releasing up to 90% of the Sr in shelf carbonates in less than 100,000 years; Morrow and Mayers, 1978; Gavish and Friedman, 1969), it can also potentially alter the Sr/Ca ratio of seawater over Quaternary cycles. The Sr flux released from exposed reefs during Quaternary sea level falls may be nearly an order of magnitude greater than the average combined riverine and hydrothermal flux of Sr to the ocean, and although the long residence time of Sr in the ocean significantly damps the ocean's response to fluctuations in the sources and sinks of Sr (Richter and Turekian, 1993), such changes in the Sr/Ca ratio of seawater may still be important in high-precision paleoceanographic studies.

The goal of this work is to investigate the effects of Quaternary sea level changes on the Sr cycle of the ocean. Coupled numerical simulations of the seawater Sr and Ca budgets are

* *Present address*: Department of Earth and Planetary Sciences, Harvard University, Cambridge, Massachusetts 02138, USA (hstoll@eps.harvard.edu).

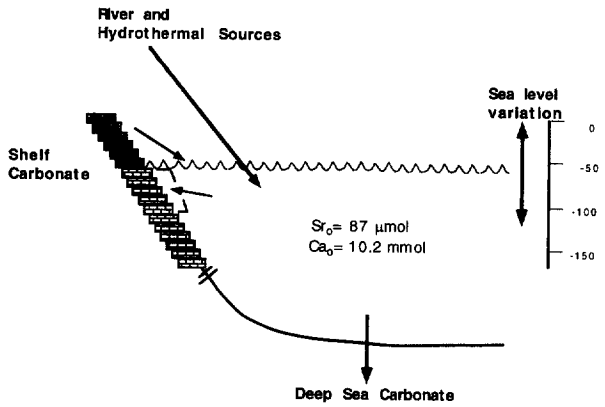

Fig. 1. Schematic of model Sr and Ca budgets. Boxes representing shelf carbonate accumulation are drawn 10 × larger to simplify figure. Boxes exposed above sea level (stippled pattern) are a source of Sr and Ca. From 0 to 50 m below sea level, boxes remove Sr and Ca from the ocean (brick pattern); boxes retain Sr and Ca when submerged at greater depths (brick pattern). Sea level variations of 120 m permit accumulation of shelf carbonate down to 170 m below modern sea level (50 m below the lowest sea level).

used to understand how different sea level histories affect the Sr cycle and to understand how glacial/interglacial changes in the carbonate budget modulate the ocean's response to changing sea levels. Investigated carbonate budget changes include variations in the ratio of shelf vs. deep sea carbonate, variations in the total amount of carbonate removed from the ocean, and periodic dissolution of shelf carbonates. A sensitivity analysis of basic model parameters, including the mean carbonate deposition rate, and the extent and rate of recrystallization of shelf aragonites, is also conducted. We then consider the implications of variations in the Sr cycle for Sr/Ca paleotemperature determinations in corals (Beck, 1992; Guilderson et al., 1994) and assess the potential for variation in the strontium isotopic composition of seawater. Finally, we evaluate the potential for detecting the modeled Sr/Ca fluctuations in the Quaternary sediment record.

2. MODEL

2.1. Simulation of Ocean Strontium and Calcium Budgets

Our numerical approach is to use a simple box model to simulate the Sr and Ca budgets of the ocean (Fig. 1) and track the concentration of Sr and Ca in the ocean over time. The relevant mass conservation equations for Ca and Sr in the ocean are given by

$$dCa/dt = J_{Ca}riv + J_{Ca}diss - Jcarb \quad (1)$$

$$dSr/dt = J_{Sr}riv + J_{Sr}rxlln + J_{Sr}diss - Jcarb*(Xshelf*D_{Srshelf} + (1-Xshelf)*D_{Srdeep}) \quad (2)$$

where J_{Ca}riv represents influxes of Ca from combined river and hydrothermal sources, J_{Ca}diss represents influxes of Ca from dissolution of shelf carbonates, and Jcarb is the accumulation rate of carbonate sediment. J_{Sr}riv, J_{Sr}rxlln, and J_{Sr}diss represent influxes of Sr from combined river and hydrothermal sources, recrystallization of shelf carbonates, and dissolution of shelf carbonates, respectively. Xshelf is the fraction of carbonate accumulating in the shelf environment, and $D_{Srshelf}$ and D_{Srdeep} are the mean Sr distribution coefficients for carbonates accumulating in shelf and deep sea environments. In the model, we do not explicitly define the mineralogy of shelf vs. deep sea carbonates, but instead use average Sr/Ca distribution coefficients based on geochemical data for the bulk carbonate in each environment (Roselle, 1985; Schlanger, 1988; Hess et al., 1986).

The inventory of Sr and Ca in shelf carbonates is also tracked through time. Mass conservation equations for Sr and Ca in shelf carbonate are given by

$$dCa/dt = Jcarb*Xshelf - J_{Ca}diss \quad (3)$$

and

$$dSr/dt = Jcarb*Xshelf*DSrshelf - J_{Sr}rxlln - J_{Sr}diss \quad (4)$$

In the model, shelf carbonate accumulation is uniformly distributed in boxes located between sea level and 25–50 (H_{shelf}) m below sea level. We do not weight the accumulation by hypsographic area so that we can investigate the sensitivity of the result to the depth of shelf carbonate accumulation.

Fluxes of Sr from recrystallization and fluxes of Sr and Ca from dissolution result from exposure of shelf carbonate boxes above sea level. Recrystallization results in a first order exponential decrease of the Sr content of exposed boxes and no change in the Ca content of exposed boxes. Integrating Sr losses from boxes at all exposed depths yields the recrystallization flux to the ocean. Dissolution of carbonate results in a linear decrease in the Sr and Ca content of exposed boxes; integrating Sr and Ca losses over all the boxes yields the dissolution fluxes to the ocean, which reaches a maximum value of $Jdiss_{max}$ at glacial maxima.

The fluxes of Sr and Ca from river and hydrothermal sources are assumed to remain constant throughout the simulation. The total carbonate flux may vary with sea level in the model simulation according to the following equation:

$$Jcarb = (SL - SL_{avg})/SL_{avg}*Jcarb_{avg}*A_{carb} \quad (5)$$

where SL is sea level and SL_{avg} the mean sea level over the course of the simulation, and A_{carb} defines the amplitude of variation. The distribution of carbonate in shelf and deep sea environments varies with the rate of change of sea level. Sea level rises at moderate rates (5–15 m/ky) lead to maximum shelf accumulation rates (Xshelf max), where Xshelfmax and Xshelfmin represent maximum and minimum fractions of carbonate accumulation (Jcarb) occurring in the shelf environment. As the rate of sea level rise goes from 5 to −5 m/ky, shelf accumulation rates decrease linearly from Xshelfmax to Xshelfmin. As the rate of sea level rise increases to very rapid rates (15–25 m/ky), shelf accumulation also decreases linearly from Xshelfmax to Xshelfmin. At rates of sea level fall greater than 5 m/ky (−5 m/ky) and rates of rise greater than 25 m/ky, we assume that shelf carbonate accumulation is insignificant.

The model is initialized with modern Sr and Ca concentrations. Because the model requires data on the fraction of carbonate accumulating in shelf vs. deep sea settings in order to evaluate the partitioning of Sr, we parameterize the model

Table 1. Summary of model parameters and values used in model simulations. Parameters used in the control simulation are shown in boldface text. References are given in the text.

Parameter	Description	Values
Sr_o	Initial Sr concentration	87 umol/L
Ca_o	Initial Ca concentration	10.2 mmol/L
D_{Srdeep}	Sr partitioning in deep sea carbonate	0.176
$D_{Srshelf}$	Sr partitioning in shelf carbonate	0.9
$J_{Sr}riv$	River/Hydrothermal Sr influx to ocean	to balance budget
$J_{Ca}riv$	River/Hydrothermal Ca influx to ocean	to balance budget
$Jcarb_{avg}$	Mean carbonate accum. rate	1.6 to **2.0E13** mol/
$Xshelf_{avg}$	Mean fraction of carbonate accumulation in shelf	0.4
$Xshelf_{max}$/ $Xshelf_{min}$	Maximum /minimum fraction of carbonate accumulation in shelf	**0.85/0.0** 0.70/0.15 1.00/0.00
A_{carb}	Amplitude of variation in total carbonate accumulation rate	**0** to 0.20
τ_{rxlln}	Half decay time of shelf recrystallization	10 to 40 ky (**20 ky**
X_{rxlln}	Extent of shelf recrystallization	0.7 to **0.9**
H_{shelf}	Thickness of shelf accumulation zone (m below sea level)	25 to **50** m
$Jdis_{max}$	Maximum glacial shelf carbonate dissolution flux	**0** to 0.4E13 mol/yr

fluxes using the carbonate removal rates and adjust the river/hydrothermal Sr and Ca fluxes to attain long term balance for each simulation. The drift in Sr and Ca concentrations is less than 0.2 % over a 6 million year simulation.

2.2. Model Strategy

We analyze the behavior of Sr over Quaternary sea level cycles by setting up a control simulation with parameter choices reflecting the simplest representation of the Sr budget. In subsequent simulations, we alter parameters individually to examine how different sea level histories and carbonate budget parameters modify the basic response observed for the control case. We do not suggest that the control parameter choices are the most accurate description of the Sr and Ca budgets, merely that they represent the simplest scenario to serve as a frame of reference for our sensitivity analysis.

Data on parameter choices used in our model simulations are compiled in Table 1, with the parameters of the control simulation in boldface type. Multiple values given for a parameter indicate the range of sensitivity investigated for that parameter. In the following section, we discuss in detail the available constraints on model parameters and the rationale for selections given in Table 1.

2.3. Model Parameters

2.3.1. Sea level forcing

To test the sensitivity of the model to details of the sea level history, we simulate sea level change in two ways. First, we use the benthic foraminiferal $\delta^{18}O$ record in Site V19-30 (Shackleton and Pisias, 1985). We also use a curve based on precise dating and altimetry of Pacific reef terraces (Chappell and Shackleton, 1986; Chappell et al., 1996). The first 120 ky of each record are repeated to generate a longer sequence, and both curves are normalized to a sea level drop of 120 m during the last glacial maximum (Fairbanks, 1989). The main difference between the sea level curves is that the reef altimetry curve has higher sea levels during interstadials, as shown in Fig. 2, so the mean sea level of the reef altimetry curve is −54 m while that of the benthic $\delta^{18}O$ curve is −70 m. For the control simulation, the benthic $\delta^{18}O$ record is used to force model sea level.

2.3.2. Carbonate deposition

A realistic representation of the Sr budget of the ocean requires knowledge of several aspects of the carbonate budget, including the average rate of carbonate removal from the ocean and the average partitioning of carbonate between shelf and deep sea regimes, as well as the variability of the total carbonate accumulation rate and the variability of basin/shelf partitioning. As several of these parameters are difficult to measure and several different carbonate budgets have been proposed, we undertake a sensitivity analysis across a range of estimated values. We require that all carbonate budgets balance over glacial cycles, as suggested by Milliman (1993), and Opdyke and Walker (1992).

Not surprisingly, there is less uncertainty in estimates of long term average carbonate fluxes than in estimates of modern fluxes or past minimum or maximum fluxes. Estimates of total mean carbonate accumulation rates during the Quaternary range from 1.8×10^{13} mol/yr (Holland, 1984; Hay and Southam, 1977) to 2.0×10^{13} mol/yr (Opdyke and Walker, 1992); these rates are consistent with a long-term steady-state given estimated Ca influxes of 1.9×10^{13} mol/yr (Berner and Berner, 1996) to 2.1×10^{13} mol/yr (Milliman, 1993). Over the Quaternary, approximately 40% of this carbonate accumulates in the shelf environment, based on a long term average Plio-Pleistocene shelf accumulation rate of 0.8×10^{13} mol/yr (Opdyke and Wilkinson, 1988) and average Quaternary deep sea

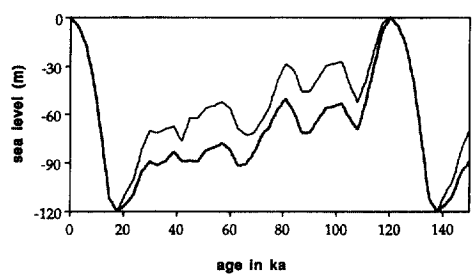

Fig. 2. Sea level curves for the last 150 ka derived from benthic $\delta^{18}O$ record (Shackleton and Pisias, 1985; lower curve) and altimetry and dating of Pacific reef terraces (Chappell and Shackleton, 1986; Chappell et al, 1996; upper curve). Sea level in meters relative to present sea level.

accumulation rates of 1.2 to 1.3 $\times$ 10^{13} mol/yr (Davies and Worsley, 1981). In our simulations, we use a maximum value of 2.0 $\times$ 10^{13} mol/yr for the mean total carbonate accumulation rate (J_{carb}avg) , and a conservative minimum value of 1.6 $\times$ 10^{13} mol/yr slightly lower than the minimum estimates. We use a value of 0.4 for the average fraction of the carbonate flux partitioned to the shelf environment ($Xshelf_{avg}$). For the control simulation, we use an average total carbonate accumulation rate of 2.0 $\times$ 10^{13} mol/yr.

Carbonate accumulation rates for the Holocene exceed the long term average. Berner and Berner (1996) estimated that present carbonate accumulation is 2.4 $\times$ 10^{13} mol/yr, 20% higher than the mean carbonate accumulation rate. We adopt the 20% amplitude of variation in total carbonate outflux (A_{carb}) suggested by the Berner and Berner (1996) data and also compare this result with a calculation using a constant carbonate removal flux. The constant carbonate removal rate is used in the control simulation.

Higher Holocene carbonate accumulation rates reflect accelerated accumulation of shelf carbonates, likely resulting from moderate rates of sea level rise during the Holocene which have accommodated extensive reef development (Hay and Southam, 1977). Recent modeling of reef habitat changes over glacial cycles also suggests that glacial shelf carbonate accumulation rates were probably restricted to no more than 27% of today's rates (Kleypas, 1997). According to models of Walker and Opdyke (1995), elevated shelf carbonate accumulation decreases the alkalinity of seawater and consequently reduces the preservation of deep sea carbonates so that variations in shelf and deep sea carbonate accumulation rates are out of phase. Sediment data of Farrell and Prell (1991) and Francois et al. (1990) do suggest general lysocline shoaling and lower Holocene carbonate mass accumulation rates, although the spatial distribution of these changes has not been rigorously explored. Consistent with these observations, our model varies shelf and deep sea accumulation rates by varying the fraction of total sedimentation in the shelf environment (X_{shelf}) with the rate of sea level change, following Walker and Opdyke (1995). Estimates of Holocene shelf carbonate accumulation rates range from in excess of 1.3 $\times$ 10^{13} mol/yr (Hay and Southam, 1977) to as high as 1.8 to 2.3 $\times$ 10^{13} mol/yr (Opdyke and Walker, 1992). High carbonate accumulation rates can be reconciled with mean average carbonate accumulation rates and average partitioning of 40% of carbonate in the shelf environment using several choices of maximum and minimum fraction of carbonate in the shelf environment ($Xshelf_{max}$/$Xshelf_{min}$). We run the model using $Xshelf_{max}$/$Xshelf_{min}$ values of 0.85/0 and 0.70/0.15. Because the total carbonate accumulation rates and the average sea level vary for different simulations, the actual mean Holocene fluxes of shelf carbonate implied by these $Xshelf_{max}$/$Xshelf_{min}$ values varies from 1.2 to 1.6 $\times$ 10^{13}. For the control run, we use $Xshelf_{max}$/$Xshelf_{min}$ values of 0.85/0.

The carbonate parameters used in our model differ somewhat from those of Milliman (1993), who estimated both modern and glacial rates of deep sea and shelf carbonate accumulation but whose budget did not balance over glacial cycles. Milliman (1993) suggested modern shelf and deep sea fluxes of 1.7 and 1.5 $\times$ 10^{13} mol/yr, respectively, and glacial fluxes of 0.1 and 1.5 $\times$ 10^{13} mol/yr in the shelf and deep sea, respectively. To attain a balanced budget, at least one of these rates must be reduced. Since the shelf fluxes are within the range of estimates of other workers, we suggest that deep sea carbonate fluxes are overestimated either for the modern or for the last glacial. Assuming lower glacial deep sea accumulation rates (0.31–0.97 $\times$ 10^{13} mol/yr to balance using different sea level curves) implies a large imbalance between glacial and Holocene carbonate accumulation rates, with modern accumulation rates exceeding the long term average of Opdyke and Walker (1992) by 65% (A_{carb}). Assuming lower modern deep sea accumulation rates (0.5–0.8 $\times$ 10^{13} mol/yr to balance using different sea level curves), the assumption favored by Milliman and Droxler (1996), implies a budget more consistent with the one we chose. The imbalance between glacial and Holocene carbonate accumulation rates in this case is much lower, with modern accumulation rates exceeding the long term average of Opdyke and Walker (1992) by 15–30% (A_{carb} differs slightly for different sea level forcings), similar to our estimate of 20%. Both assumptions imply average partitioning of 35% of carbonate in the shelf environment (X_{shelf}), again similar to our choice of 40%.

2.3.3. *Aragonite recrystallization on exposed continental shelves*

Morrow and Mayers (1978) demonstrated that the Sr/Ca ratio of recrystallized shelf carbonates is 75–90% lower than the original carbonate, in agreement with earlier estimates of Harris and Matthews (1968), and consistent with the large decrease in partitioning coefficients from biogenic aragonite (DSr = 1.0) to inorganic calcite (DSr = 0.03). Data of Gavish and Friedman (1969) indicate that the amount of aragonite in exposed shelf carbonates decreases exponentially with time with a decay constant of 6.9 to 13.0 $\times$ 10^{-2}/ ky The corresponding Sr loss in these sediments is slightly slower, with a decay constant of 1.7–6.9 $\times$ 10^{-2}/ k.y. Because only aragonite recrystallizes, but our shelf sediment is not exclusively aragonite, we limit the maximum extent of recrystallization of shelf carbonates (X_{rxlln}) by allowing subaerially exposed shelf carbonate to release a maximum of 70–90% of its original Sr. The rate of release is proportional to concentration, following first order linear kinetics with a maximum and minimum recrystallization rates given by decay constants of 6.9 $\times$ 10^{-2}/ k.y and 1.7 $\times$ 10^{-2}/ k.y., respectively (t_{rxlln} from 10 to 40 ky). For the control run, we take X_{rxlln} to be 0.9 and t_{rxlln} to be 20 ky.

The recrystallization flux is also dependent on the depth range of shelf carbonate accumulation, H_{shelf}, as this parameter determines the rate at which shelf carbonate is exposed by sea level falls. Boggs (1987) suggested that deposition of shelf carbonate was restricted to 0–50 m below sea level, and this value is used for most of the simulations. Recent work by Kleypas (1997) suggests that most carbonate deposition may occur between 0 and 25 m below sea level, with steeply diminishing accumulation below 25 m. For comparison, we also run one simulation with shelf accumulation restricted to 0–25 m, which provides a maximum rate of exposure of shelf carbonate during sea level falls. In the control run, we use an H_{shelf} value of 50 m.

Strontium released from recrystallizing shelf carbonates is assumed to be mixed homogeneously into the ocean with no

mass transfer limitation. This assumption is supported by the lack of any significant gradient (>1 %) in the Sr/Ca ratio of surface seawater between modern coral reef waters and open ocean waters (deVilliers et al., 1994).

We neglect any shelf carbonate exposure which may result from local tectonic uplift because the rate of uplift is slow relative to the rate of Quaternary sea level changes, and the long term effects of uplift are approximately balanced by those of subsidence in other regions.

2.3.4. *Dissolution and chemical erosion of previously deposited carbonates*

The effect of dissolution of exposed shelf carbonates is also investigated in this model. Estimates of shelf dissolution fluxes vary widely. Schlanger (1988) suggests a dissolution flux on the order of 0.3×10^{13} mol/yr during maximum shelf exposure at glacial lowstands, based on observations of the modern limestone removal rate per area in karst regions. Walker and Opdyke (1995) suggest that shelf carbonate dissolution fluxes may reach 2.0×10^{13} mol/yr during maximum glacial lowstands; however, this flux is calculated as a fit parameter to achieve the full amplitude glacial pCO_2 drop from the Coral Reef Hypothesis. As the coral reef hypothesis need not be the only cause of glacial pCO2 changes, the proposed dissolution flux is likely inflated. For this reason, in models including shelf dissolution, we use maximum shelf dissolution fluxes ($Jdis_{max}$) of 0.3 to 0.8×10^{13} mol/yr, more consistent with the estimates of Schlanger (1988). In order to maintain long term net removal of 40% of carbonate in the shelf setting, these dissolution fluxes require $Xshelf_{max}/Xshelf_{min}$ values of 0.90/0 and 1.00/0. In the control simulation, we assume negligible shelf dissolution ($Jdis_{max} = 0$).

We do not explicitly include a flux from chemical erosion of deep sea carbonates because the Sr/Ca ratio of chemically eroding deep sea carbonates is very nearly identical to that of carbonate being deposited and, therefore, equivalent to a reduction in the deep sea carbonate accumulation rate. The long term flux of Sr from diagenesis of carbonate sediments is also small (Richter and Liang, 1993; Baker et al., 1982) and not included here as a separate flux.

2.4. Balancing Strontium and Calcium Budgets

Because we use the river and hydrothermal sources as a tuning parameter to balance model Sr and Ca budgets, comparing the model-required fluxes with estimated fluxes provides a check on whether our model budgets are reasonable. Uncertainties in the Sr and Ca hydrothermal flux produce a wide range of estimates for the rate of addition of these elements to the ocean. Estimates for the total Sr addition from rivers and hydrothermal sources range from 3.2×10^{10} mol/yr (Hodell et al., 1989) to 5.1×10^{10} mol/yr (Palmer and Edmond, 1989). Most recent estimates of the Ca flux are around 2×10^{13} mol/yr (e.g., Berner and Berner, 1996; Milliman, 1993).

Our assumption of a constant riverine and hydrothermal influx is probably not accurate due to variation in the river flux of Sr and Ca to the ocean over glacial cycles (e.g,. Mortlock et al., 1992). However, changes in the river flux even by a factor of 2 or 3 are second order relative to flux changes due to shelf weathering and, therefore, have a minimal effect on the Sr/Ca ratio of seawater.

As Schlanger (1988) noted previously, modern rates of Sr removal in shelf and deep sea carbonates significantly exceed estimated rates of Sr addition from river and hydrothermal fluxes. In order to balance the long term Sr budget in our simulations, we use Sr influxes which are 50–60% lower than the mean gross rate at which Sr is partitioned into carbonates. The median influx to balance the model is 3.6×10^{10} mol/yr. These lower influxes are required because Sr is extensively recycled to the ocean from shelf aragonites during glacial sea level falls. Aragonite accumulation is merely a temporary Sr reservoir which is largely recycled over the 100 ky timescales of glacial sea level change, while calcite serves as more permanent repository of Sr. Consequently, during times of frequent sea level changes, the Sr budget is rarely balanced on timescales less than several hundred thousand years.

In contrast to Sr, Ca is not significantly recycled from deep sea or shelf carbonate reservoirs on short timescales. If there is no shelf carbonate dissolution flux, the Ca budget is balanced when the combined river and hydrothermal inputs equal the average carbonate removal rate. Even in the case of maximum shelf carbonate dissolution fluxes of 0.3 to 0.8×10^{12} mol/yr, less than 10% of the Ca removed from the ocean is recycled over the timescale of glacial cycles.

3. RESULTS AND DISCUSSION

3.1. Response of Strontium to Pleistocene Sea Level Changes

3.1.1. *Control simulation*

The basic behavior of the model is illustrated in Fig. 3, using the parameters of our control simulation. Sea level variations lead to periodic fluctuations in the Sr/Ca ratio of seawater on the order of a few percent over Quaternary glacial cycles (Fig. 3 a,b). The Sr/Ca ratio increases rapidly during glacial maxima, peaks approximately 3 ky after the glacial maxima, and returns gradually to pre-glacial values. The phase lag and slow decrease of the Sr/Ca ratio are due to the long residence time of Sr in seawater (see Richter and Turekian, 1993).

Changes in Sr fluxes responsible for Sr/Ca variations are shown in Fig. 3c and 3d. The ratio of carbonate sedimentation in shelf vs. deep sea environments depends on the rate of change of sea level, with increased shelf carbonate accumulation occurring during periods of sea level rise (Fig.3c). However, a comparison of Fig. 3c with 3a shows that these increases have little direct effect on the Sr/Ca ratio of seawater. Instead, it is the addition of Sr from recrystallizing shelf carbonates during sea level falls which produces the variation in the Sr/Ca ratio (Fig. 3d). The relationship between sea level falls and the shelf recrystallization flux is not straightforward, as a comparison of Fig. 3a and 3d illustrates. Most important in modulating the Sr response to sea level change is the position of sea level relative to the depth where Sr is sequestered in shelf carbonate. Figure 4a shows the steady-state inventory of Sr in shelf carbonate for the last 150 ky of model simulation. The inventory is shown for three different depth ranges: 0–40, 41–80, and 81–120 m below modern sea level. As this figure indicates, throughout the last 150 ka, the majority of shelf carbonate Sr is

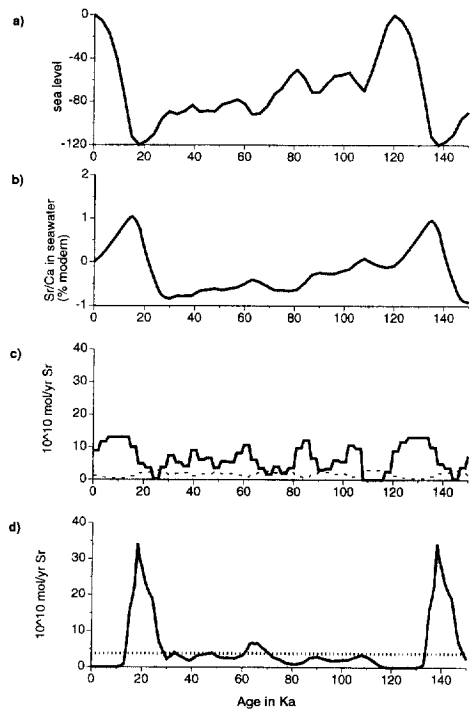

Fig. 3. Results from control simulation showing variation in seawater Sr/Ca ratio and Sr fluxes for the last 150 ka. Control simulation parameters described in text. (a) Sea level curve derived from benthic $\delta^{18}O$ record of Shackleton and Pisias (1985). (b) Variation in Sr/Ca ratio of seawater, plotted as the percent difference from the modern Sr/Ca ratio of 8.52 mmol/mol. (c) Carbonate removal of Sr from the ocean via shelf carbonate (heavy line) and deep sea carbonate (dashed line). (d) Addition of Sr to the ocean via a combined river and hydrothermal flux (dashed line) and shelf recrystallization (heavy line).

sequestered in deeper regions between −80 and −120 m, which are submerged at depths of shelf accumulation through much of the sea level history and exposed only for short time intervals. In contrast, shallower regions are submerged at depths of reef accumulation for only short periods, and accumulate very little Sr for weathering during sea level falls. Consequently, the large (70 m) interstadial sea level fall at 120 ka, and the smaller fall at 100 ka, expose very little shelf carbonate Sr. The resulting Sr recrystallization fluxes (Fig. 4b) are smaller than the combined river and hydrothermal influx and produce only minor inflections in the Sr/Ca ratio of seawater (Fig. 3 d,b). The sea level fall at 65 ka is able to tap some of the deeper Sr reserves and produces a slightly larger flux, but only the final sea level fall at 30 ka exposes the large Sr inventory between −80 and −120 m and results in a large Sr flux. This pulse of Sr, nearly an order of magnitude greater than the combined river and hydrothermal influx, is responsible for the large increase in the Sr/Ca ratio of seawater seen in Fig. 3b.

We further our understanding of the behavior of Sr in seawater over Quaternary glacial cycles by examining how different sea level and carbonate budget parameters modulate the basic response discussed for the control case. This is accomplished through a series of simulations, the results of which appear in Table 2. Initially, we examine the model sensitivity to basic parameter choices (Table 2, Runs 1–5). Subsequently, we investigate the effects of variations in the sea level history and carbonate budget (Runs 6–15). Finally, using the results of the previous simulations, we choose parameters to maximize and minimize variation in the Sr/Ca ratio of seawater overall and since the last glacial maximum (Runs 16–19).

3.1.2. *Sensitivity analysis of basic parameters*

Basic parameter choices such as the mean carbonate deposition rate and the extent and rate of recrystallization of shelf aragonites exert a strong influence on the magnitude of Sr/Ca variations. Lower total carbonate accumulation rates (1.6×10^{13} vs. 2.0×10^{13} mol/yr) reduce Sr/Ca variations (1.88 vs. 1.50 %; Runs 1 vs. 2). This results from the increased residence time of Sr in the ocean which more strongly damps the amplitude of the ocean's response to flux changes (e.g., Richter and Turekian, 1993).

Reduced Sr loss during recrystallization (70% vs. 90%) decreases the amplitude of Sr/Ca variations (1.88 vs. 1.5 %; Run 1 vs. 3). The rate of recrystallization also has an effect on the amplitude of Sr/Ca variations. More rapid recrystallization rates result in lower total Sr/Ca amplitudes because more Sr is released from shelf carbonates during brief interstadial sea level falls, leaving less Sr for release during glacial maxima (1.77 vs. 1.95%; Run 4 vs. Run 5). However, more rapid recrystallization rates increase the amplitude of Sr/Ca variation since the last glacial maximum. More rapid release of Sr reduces the duration of the Sr pulse, permitting the Sr/Ca ratio to decrease more rapidly following shelf exposure (1.08 vs. 0.99 %; Run 4 vs. Run 5). Decreasing the thickness of the zone of shelf accumulation from 50 to 25 m is analogous to increasing the recrystallization rate, in that it decreases the total amplitude of Sr/Ca variations (1.77 vs. 1.88%, Run 1 vs. Run 6), but increases the amplitude of Sr/Ca variation since the last glacial maximum (1.12 vs. 1.04).

3.1.3. *Response to different sea level histories*

Although all sea level curves are normalized to the same amplitude, differences in the shapes of the sea level curves lead to different model Sr/Ca responses. For the same choices of carbonate parameters, the sea level curve derived from reef altimetry produces a greater total amplitude of Sr/Ca variation than the curves derived from the benthic $\delta^{18}O$ record (2.41 vs. 1.88%, Runs 7 vs. 1; 2.12 vs. 1.7%, Runs 9 vs. 8; and 2.31 vs. 1.73%, Runs 13 vs. 12). This amplitude difference results from higher interglacial sea levels in the reef altimetry curve in contrast to the larger initial sea level fall between 120 and 100 ky in the benthic $\delta^{18}O$ curve (Fig. 2). As a result, between 120 and 80 ka, the amount of Sr released from shelf recrystallization is 50% higher with the benthic $\delta^{18}O$ curve than with the reef altimetry curve, where shelf Sr is more effectively sequestered. The more continuous release of shelf Sr with the benthic $\delta^{18}O$ curve reduces the amplitude of Sr/Ca variations.

3.1.4. *Response to temporal and spatial variations in carbonate deposition*

Temporal variations in the amount of carbonate removed from the ocean, as well as variation in the locus of carbonate removal, also affect the amplitude of seawater Sr/Ca variations. Strontium variations are enhanced by variable carbonate re-

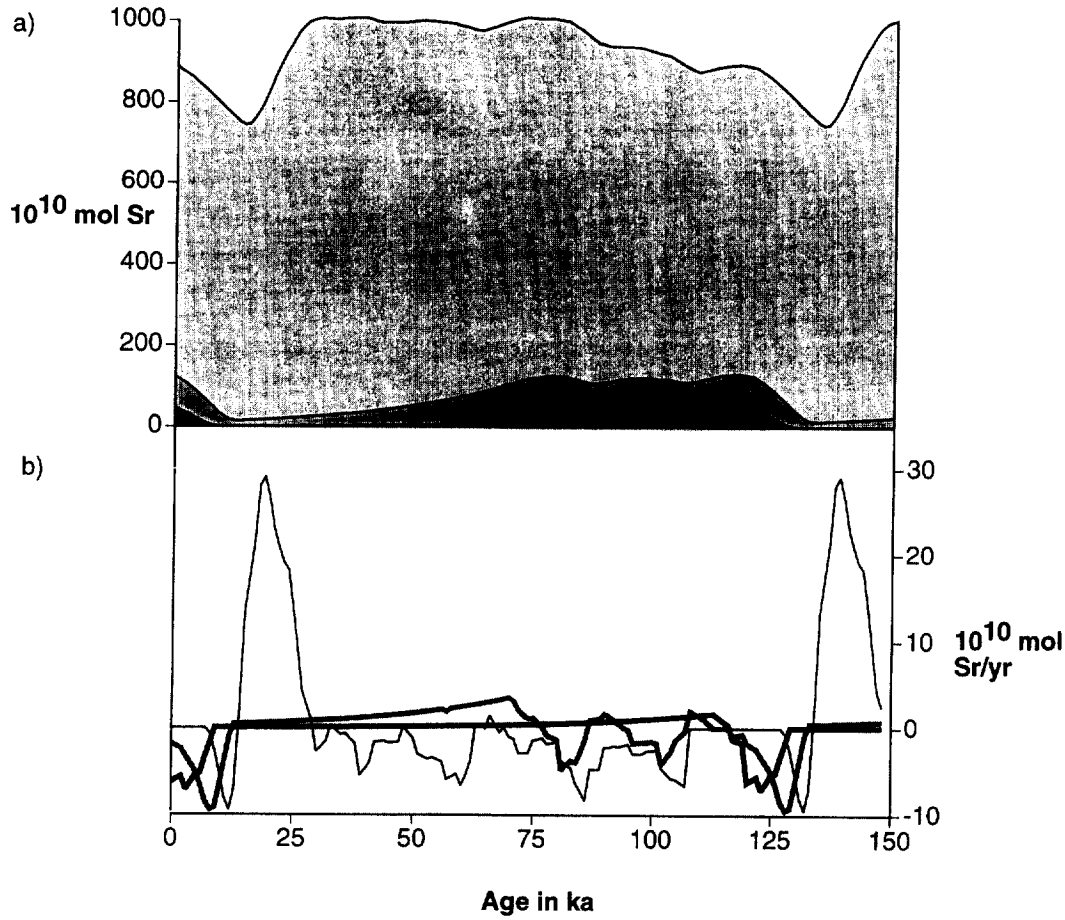

Fig. 4. Strontium inventory and fluxes in shelf carbonate for the control simulation. (a) Inventory of shelf carbonate Sr through time, integrated over depths from 0–40 (black), 41–80 (dark gray) , and 81–120 m (light gray) below modern sea level. (b) Flux of Sr from shelf carbonate through time, integrated over depths 0–40 (thick black line), 41–80 (thick gray line) , and 81–120 m (thin black line) below modern sea level. Positive fluxes represent recrystallization fluxes of Sr from shelf carbonates to the ocean; negative fluxes represent removal of Sr from the ocean during shelf carbonate accumulation.

moval because carbonate accumulations are higher during the time when most carbonate removal occurs in the shelf environment, and a greater fraction of Sr is sequestered there and available for subsequent weathering. However, variation in carbonate removal also produces fluctuations in the Ca concentration of seawater which are concurrent with Sr variations (Fig. 5). The net effect is that variable rates of carbonate deposition result in lower amplitudes of Sr/Ca variation (2.41 vs. 2.12 %, Runs 7 vs. 9; 1.88 vs. 1.70 %, 1 vs. 8).

Variation in the amount of shelf vs. deep sea carbonate accumulation also affects the Sr budget. However, as Table 2 demonstrates, the largest rates of recent shelf accumulation proposed by Opdyke and Walker (1992) (1.8 to 2.3 $\times$ 10^{13} mol/yr over the last 5 ka) cannot be reconciled with observed long term averages (0.8 $\times$ 10^{13} mol/yr) without significant shelf carbonate dissolution. Without dissolution, the largest rate which can balance to the long term average is 1.4 $\times$ 10^{13} mol/yr for constant carbonate accumulation and 1.7 $\times$ 10^{13} mol/yr for variable carbonate accumulation. Only with shelf dissolution fluxes of 0.3 to 0.8 $\times$ 10^{13} mol/yr are shelf accumulation rates within the estimates of Opdyke and Walker (1992).

With no shelf dissolution, different maximum shelf accumulation rates have no effect on the total amplitude of Sr/Ca variation because the amount of Sr available for weathering during glacial maxima is unchanged (Runs 1 vs. 10; 7 vs. 11). However, the magnitude of Sr/Ca variation since the last glacial maximum is larger for higher maximum shelf accumulation rates because the more extensive shelf carbonate sedimentation immediately following the last glacial maximum pulse of Sr/Ca more efficiently reduces the seawater Sr/Ca ratio (1.04 vs. 0.84%, runs 1 vs. 10; 0.99 vs. 0.77%, runs 8 vs. 11).

Shelf dissolution permits greater pre-glacial accumulation of shelf carbonates than would otherwise be possible without exceeding long term average accumulation rates. Consequently, a larger amount of Sr is available for release during lowstands. Because the rate of aragonite recrystallization, which releases only Sr, is greater than the rate of dissolution, which releases Ca in addition to Sr, shelf dissolution leads to larger Sr/Ca variations (2.20 vs. 2.12%, runs 9 vs. 13; 1.73 vs. 1.70%, runs 8 vs. 12). Variations in Sr/Ca since the last glacial maximum are also larger because increased shelf carbonate deposition following the last glacial maximum accelerates the decrease in Sr/Ca ratios by removing Sr more rapidly from the

Table 2. Results of model simulations. The first column indexes each simulation with a run number and the second column describes how the parameter choice of each simulation differs from that of the control. The third column shows the average rate of shelf carbonate accumulation over the last 5 ka, which results from parameter choice of Xshelfmax/Xshelfmin values subject to restrictions given by the long term average shelf accumulation rate. The forth and sixth columns give the resulting amplitudes of variation in the Sr/Ca ratio and Ca concentration of seawater, respectively. Amplitudes are reported as the difference between maximum and minimum percent of the modern value in a given cycle; both the total amplitude of the cycle and the decrease in Sr/Ca ratio since the last glacial maximum (LGM) are reported. The fifth column indicates the influx of Sr to the ocean required for long term balance.

Run	Description of Simulation	Shelf carbonate fluxout	Sr/Ca seawater amplitude, % modern		Sr influx	Ca seawater amplitude, % modern	
		10^13 mol/yr	Total	LGM	10^10 mol/yr	Total	LGM
Basic Parameter Sensitivity							
1	Control (parameters described in text)	1.4	1.88	1.04	3.6	0	0
2	Lower mean total carbonate accumulation rate of 1.6 x 10^13 mol/yr	1.2	1.50	0.83	2.9	0	0
3	Reduced extent of shelf carbonate Sr loss during recrystallization (70% loss)	1.4	1.50	0.94	4.6	0	0
4	Faster shelf carbonate recrystallization rate of 6.9 x 10-2/ky	1.4	1.77	1.08	3.6	0	0
5	Slower shelf carbonate recrystallization rate of 1.7 x 10-2/ky	1.4	1.95	0.99	3.7	0	0
6	Shallower zone of shelf accumulation (25 m not 50m)	1.7	1.77	1.12	2.9	0	0
Sea level and carbonate budget							
7	Chappell sea level curve	1.4	2.41	1.01	3	0	0
8	Variable carbonate accumulation rate	1.7	1.70	0.99	3.6	0.39	0.23
9	Variable carbonate accumulation rate, Chappell sea level curve	1.6	2.12	0.96	2.9	0.56	0.20
10	Reduced amplitude of variations in shelf/deep sea carbonate ratio	1.2	1.88	0.84	3.7	0	0
11	Reduced amplitude of variations in shelf/deep sea carbonate ratio variable carbonate deposition	1.4	1.70	0.77	3.6	0.39	0.23
12	Dissolution of shelf carbonate (max flux of 0.3 x 10^13 mol/y), variable carbonate deposition	2.0	1.73	1.01	3.6	0.49	0.28
13	Dissolution of shelf carbonate (max flux of 0.3 x 10^13 mol/y), variable carbonate deposition, Chappell sea level curve	2.0	2.20	0.99	2.8	0.68	0.25
14	Dissolution of shelf carbonate (max. flux of 0.8 x 10^13 mol/y),	1.7	1.93	1.06	3.7	0.36	0.15
15	Dissolution of shelf carbonate (max. flux of 0.8 x 10^13 mol/y), variable carbonate deposition	1.9	1.74	1.01	3.5	0.70	0.37
Maximum and Minimum Variations							
16	Minimize total amplitude in Sr/Ca ratio (parameters described in text)	1.1	0.99	0.56	3.6	0.31	0.19
17	Maximize total amplitude in Sr/Ca ratio (parameters described in text)	1.7	2.77	1.03	3.1	0.32	0.11
18	Minimize Sr/Ca decrease since Last Glacial Maximum (parameters described in text)	1.1	1.40	0.49	3.3	0.45	0.17
19	Maximize Sr/Ca decrease since Last Glacial Maximum (parameters described in text)	1.7	1.83	1.10	3.42	0.34	0.16

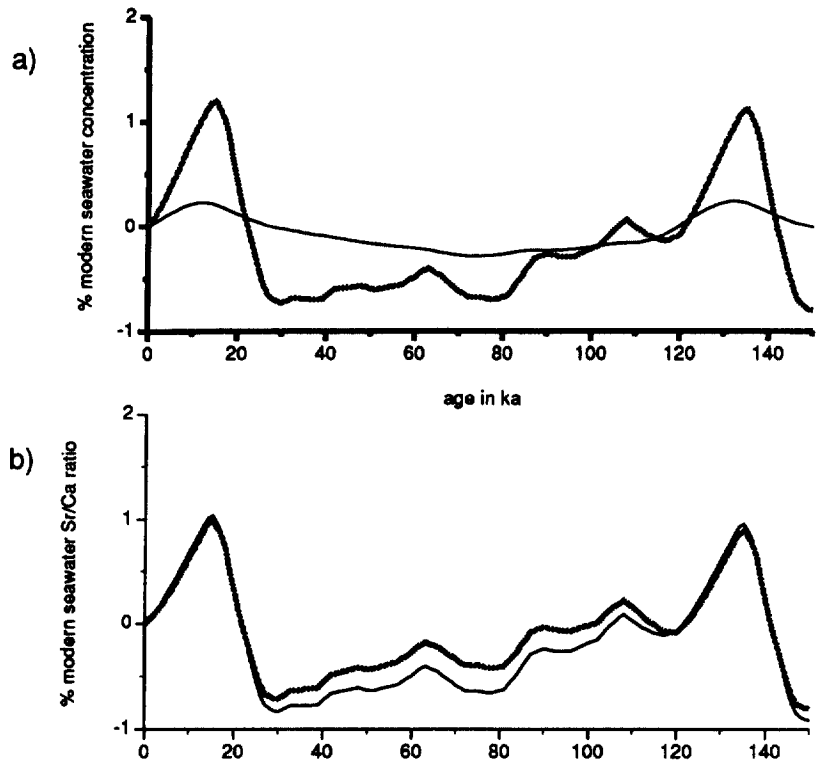

Fig. 5. Results from run with variable carbonate accumulation rates (Run #7) showing variation in seawater Sr and Ca concentrations (a) and Sr/Ca ratio (b) for the last 150 ka. Strontium (heavy line) and calcium (thin line) concentrations are plotted as percent of modern seawater concentrations of 87 mmol and 10.21 mmol, respectively. Sr/Ca ratio plotted as in Fig. 3. Heavy line is result of Run #7, thin line shows result of control for comparison.

ocean. Models forced with the reef altimetry sea level curve are much more sensitive to the additional shelf accumulation because this curve allows shelves to retain more Sr until the maximum glacial lowstand, whereas more Sr is lost from the shelves during interstadials under the benthic $\delta^{18}O$ curve.

3.1.5. Maximum and minimum variations in seawater Sr/Ca ratios

Total Sr/Ca variations are maximized by (1) a sea level history which sequesters the most Sr in shelf carbonates during interstadial periods, in this case the curve derived from reef altimetry (2) constant rates of total carbonate deposition, (3) extensive aragonite recrystallization (90% maximum) over longer timescales (rate constant of 1.7×10^{-2}/ky), and (4) carbonate budgets which include dissolution of shelf carbonates, permitting increased aragonite deposition and hence increased Sr sequestering during interstadials. Maximum and minimum total Sr/Ca variation is 2.77 % and 0.99%, respectively (Runs 16, 17). The change in Sr/Ca ratio since the last glacial maximum is maximized by the same parameter choice as for the total amplitude but with a more rapid recrystallization rate (6.9×10^{-2}/ky). The resulting Sr/Ca decrease since the last glacial maximum ranges from 1.10 (Run 18) to 0.49 % (Run 19). We can evaluate whether the Sr budget parameters for each simulation are reasonable by comparing the calculated combined riverine and hydrothermal flux necessary to balance the simulation (Table 2) with empirical estimates of the mean combined riverine and hydrothermal flux. The calculated influx from most simulations falls within the 3.2×10^{10} to 5.1×10^{10} mol/yr range suggested by Hodell et al. (1992) and Palmer and Edmond (1989), confirming that our representations of the Sr budget are reasonable. The simulations with the largest total Sr/Ca amplitudes have influxes slightly lower than 3.2×10^{10} mol/yr, possibly indicating that these simulations overestimate the importance of recycled shelf carbonate Sr in the Sr budget. Consequently, the largest Sr/Ca variations may overestimate actual variations. A more accurate range may be 0.99–1.93 % total variation in the Sr/Ca ratio of seawater. Simulations with the largest amplitudes of Sr/Ca variation since the last glacial maximum all have influxes higher than 3.2×10^{10} mol/yr, so we conclude that the full 0.49–1.10% range of decreases since the last glacial maximum is reasonable. Over both timescales, the upper end of the range probably represents the best estimate because existing evidence lends stronger support to several parameter choices which maximize the amplitude of Sr/Ca variations. First, recent data support higher total carbonate accumulation rates on the order of 2.0×10^{13} (Opdyke and Walker, 1992). In addition, the sea level curve derived from reef altimetry is more likely to reflect the actual sea level history than the benthic $\delta^{18}O$ record, which may also be influenced by temperature changes and changes in ocean circulation. Although evidence suggests that the rate of carbonate deposition varies, reducing the Sr/Ca variation, this effect may be balanced by the likely dissolution of exposed shelf carbonates, which enhances Sr/Ca variation.

The range of variation produced by our parameter choices

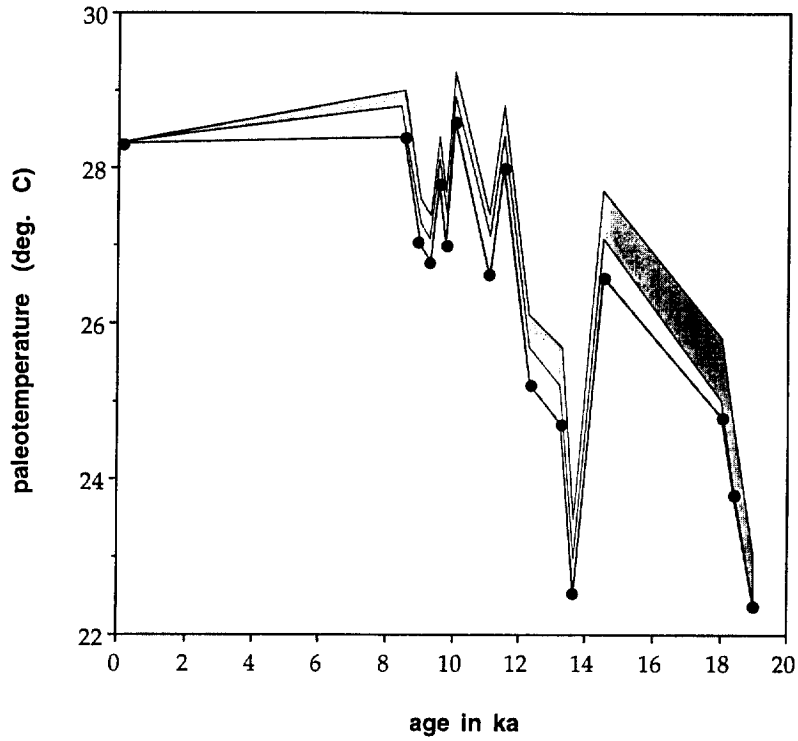

Fig. 6. Calculated coral Sr/Ca paleotemperatures since the last glacial maximum. • = Temperatures calculated by Guilderson et al. (1994) assuming constant seawater Sr/Ca ratios. Shaded region, area of temperature calculations including a correction for maximum and minimum variations in the Sr/Ca ratio of seawater predicted by our models.

does not differ significantly from simulations using the carbonate budgets of Milliman (1993). Simulations run with the both sea level forcings and the two possible balanced budgets derived from Milliman (1993) yield total Sr/Ca variations ranging from 0.84 to 1.94%.

3.2. Implications for Sr/Ca Paleothermometry in Corals

Variation in the Sr/Ca ratio of seawater has important implications for the use of Sr/Ca ratios in marine corals as a paleotemperature indicator. In corals, the partitioning of Sr into aragonite depends on the temperature at which the coral grew as well as the seawater Sr/Ca ratio. Previous workers have interpreted all temporal changes in the Sr/Ca ratio of fossil corals in terms of temperature change, assuming that the Sr/Ca ratio of seawater remained essentially constant through the Quaternary due to the relatively long residence times of these elements in the ocean (Beck et al., 1992; Guilderson et al., 1994). Based on the model results presented here, the Sr/Ca ratio of seawater may have varied by as much as 2% over glacial cycles. This change would result in apparent temperature shifts of 2–3°C, depending on the coral species.

We demonstrate the effect of seawater Sr/Ca variation by correcting the Sr/Ca paleotemperature record of Barbados corals since the last glacial maximum (Guilderson et al., 1994). In this record, the Sr/Ca ratio of Barbados corals has decreased by 5.8% (relative to modern) in the past 19 ka, which Guilderson et al. (1994) interpreted as a temperature change of 6 degrees using the Sr/Ca temperature calibration of Smith et al. (1979) for *M. verrucosa*. Using minimum and maximum estimates for the change in the Sr/Ca ratio of seawater in over the last 20 ky, we obtain corrected paleotemperatures that are up to 1.1 degrees warmer than those calculated without correcting for changing Sr/Ca ratios of seawater (Fig. 6). The largest discrepancy between corrected and uncorrected records occurs at the Allerod warming (16–14 ka) and the Younger Dryas cooling event (14–12 ka). Corrected paleotemperatures indicate that the Younger Dryas was warmer than the last glacial maximum by at least 0.5 degrees. While these corrections are relatively minor, the effects would be amplified in other corals with steeper Sr/Ca-temperature relationships and in older corals covering the last interglacial to glacial transition. For example, paleotemperature estimates from Porites would be biased by 1.5 degrees since the last glacial maximum (Alibert and McCulloch, 1997; Smith et al., 1979).

3.3. Implications for the Stronium Isotopic Composition of Seawater

The large Sr influx from shelf weathering during sea level falls can affect the strontium isotopic composition of seawater. Such an effect is possible only when the isotopic ratio of the ocean is out of equilibrium with the isotopic ratio of the riverine and hydrothermal Sr influx and the seawater $^{87}Sr/^{86}Sr$ ratio is either decreasing or increasing to reach a new steady-state value. In this situation, the large pulse of Sr from shelf recrystallization, which bears the strontium isotopic composition of the seawater at the time of carbonate deposition, dilutes the riverine and hydrothermal Sr influx by a factor of 10 or more. Such dilution briefly slows the approach of the seawater

$^{87}Sr/^{86}Sr$ ratio to equilibrium with the riverine and hydrothermal influx and transiently flattens the slope of the increasing or decreasing seawater $^{87}Sr/^{86}Sr$ ratio.

Shelf carbonate recrystallization during sea level falls may have influenced the strontium isotopic composition of seawater during the past 40 my, when high riverine $^{87}Sr/^{86}Sr$ ratios have led to disequilibrium between the isotopic composition of the Sr influx and seawater and a gradual increase in seawater $^{87}Sr/^{86}Sr$ ratios. However, in the Quaternary this is an unimportant effect because the high frequency of sea level changes relative to the change in the seawater $^{87}Sr/^{86}Sr$ ratio leads to a low contrast between seawater and shelf Sr being recycled. When we included in our model conservation equations for ^{87}Sr and ^{86}Sr (assuming that ^{86}Sr is a constant fraction of the total Sr), we found that this effect was not detectable at the ppb level of $\Delta 87Sr$, much lower than current analytical capabilities of 5–10 ppm. This result is consistent with the models of Richter and Turekian (1993) which indicated that the residence time of Sr in seawater is too large for a detectable isotopic shift on time scales less than several hundred thousand years. In contrast, the effect of shelf weathering may be significant in the Pliocene and earlier, before glaciations become frequent and regular. In this case, large sea level changes could recycle large amounts of relatively old shelf Sr possessing an isotopic composition which contrasts more strongly with that of seawater at the time of recrystallization.

3.4. Data on Quaternary Sr/Ca Variability of Seawater

Limited data exist to test our model predictions of variations in the Sr/Ca ratio of seawater over the Quaternary. Foraminiferal tests, the most commonly used material for reconstruction of past seawater chemistry, may not accurately record the Sr/Ca ratio of seawater because of vital effects. Although evidence for direct temperature dependence of Sr/Ca incorporation into foraminiferal tests remains equivocal (Delaney et al., 1985), there is strong evidence that Sr partitioning depends on Mg content (Carpenter and Lohman, 1992; Morse and Bender, 1990) which is dependent on temperature (Nurnburg et al., 1996; Opdyke et al., 1993). In addition, chemical heterogeneities in foraminiferal tests make them susceptible to selective dissolution, which can decrease Sr/Ca ratios of forams by up to 20% over a depth range of 3000 m (Brown and Elderfield, 1996). When dissolution intensity at a site varies over time, artifacts of several percent in paleo Sr/Ca records may result.

We are aware of only one published time series of Quaternary foraminiferal Sr concentrations, that of Cronblad and Malmgren (1981) from southern Indian Ocean sites E48-22 and E49-19. Both sites exhibit concurrent large variations (up to 100% increase) in the Sr concentrations of several species of planktonic foraminifera. Such changes are much too large to reflect changes in the fluxes of Sr to the ocean and must be due to vital and/or selective dissolution effects. While it may be possible to correct foraminiferal data for dissolution and temperature effects, the predicted size of the change in the Sr/Ca ratio of seawater (1–2%) is likely too small to accurately measure in this way.

4. CONCLUSIONS

Although Sr has a long residence time in the ocean, short term variations in seawater Sr concentrations are still possible if there are large perturbations in fluxes such as those produced by Quaternary sea level variations. Model simulations predict that the Sr/Ca ratio of seawater varies by 1–2 % over Quaternary glacial cycles. Such variation is sufficient to produce up to 3°C errors in paleotemperatures calculated from coral Sr/Ca ratios. Changes in the Sr budget during Quaternary sea level cycles are not sufficiently large to affect the strontium isotopic composition of seawater. Unfortunately, effects of temperature and dissolution on the incorporation and preservation of seawater Sr/Ca ratios in foraminiferal tests appear to preclude measurement of seawater Sr/Ca variations at this level of precision.

Acknowledgments—This work was partly supported by an Office of Naval Research Graduate Fellowship to Stoll. We thank Karl Turekian and two anonymous reviewers for helpful suggestions on the organization of this manuscript.

REFERENCES

Alibert C. and McCulloch M.T. (1997) Strontium/calcium ratios in modern Porites corals from the Great Barrier Reef as a proxy for sea surface temperature: Calibration of the thermometer and monitoring of ENSO. *Paleoceanography* **12**, 345–363.

Baker P., Gieskes J. M., and Elderfield H. (1982) Diagenesis of carbonates in deep-sea sediments—evidence from Sr/Ca ratios and interstitial dissolved Sr^{+2} data. *J. Sediment. Petrol.* **52**, 52–71.

Beck J. W. et al. (1992) Sea-surface temperature from coral skeletal strontium/calcium ratios. *Science* **257**, 644–647.

Berner E. and Berner R. (1996) *Global Environment: Water, Air, and Geochemical Cycles*. Prentice Hall.

Boggs S. J. (1987) *Principles of Sedimentology and Stratigraphy*. Merrill.

Brown S. J. and Elderfield H. (1996) Variations in Mg/Ca and Sr/Ca ratios of planktonic foraminifera caused by postdepositional dissolution: Evidence of shallow magnesium-dependent dissolution. *Paleoceanography* **11**, 543–551.

Capo R. C. and DePaolo D. J. (1990) Seawater strontium isotopic variations from 2.5 million years ago to the present. *Science* **249**, 51–55.

Carpenter S. J.and Lohman K. C. (1992) Sr/Mg ratios of modern marine calcite: Empirical indicators of ocean chemistry and precipitation rate. *Geochim. Cosmochim. Acta* **56**, 1837–1849.

Chappell J. et al. (1996) Reconciliation of late Quaternary sea levels derived from coral terraces at Huon Peninsula with deep sea oxygen isotope records. *Earth Planet. Sci. Lett.* **141**, 227–236.

Chappell J., and Shackleton N. J. (1986) Oxygen isotopes and sea level. *Nature* **234**, 137–139.

Cronblad H. G., and Malmgren B. A. (1981) Climatically controlled variation of strontium and magnesium in Quaternary planktonic foraminifera. *Nature* **291**, 61–64.

Davies T.A., and Worsley, T.R.(1981) Paleoenvironmental implications of oceanic carbonate sedimentation rates. *Soc. Econ. Paleontol. Spec. Publ.* **32**, 169–179.

De Villiers S., Shen G. T., and Nelson B. K. (1994) The Sr/Ca-temperature relationship in coralline aragonite: Influence of variability in (Sr/Ca) seawater and skeletal growth parameters. *Geochim. Cosmochim. Acta* **58**, 197–208.

Delaney M. L., Be A. W. H., and Boyle E. A. (1985) Lithium, strontium, magnesium, and sodium in foraminiferal calcite shells from laboratory culture, sediment traps, and sediment cores. *Geochim. Cosmochim. Acta* **49**, 1327–1341.

Fairbanks R. C. (1989) A 17,000-year glacio-eustatic sea level record: influence of glacial melting rates on the Younger Dryas event and deep-ocean circulation. *Nature* **342**, 637–642.

Farrell J.W., and Prell W.L. (1991) Pacific $CaCO_3$ preservation and

$\delta^{18}O$ since 4 Ma: Paleoceanic and paleoclimatic implications. *Paleoceanography* **6**, 485–498.

Francois R., Bacon M. P., and Suman D. O. (1990) Thorium 230 profiling in deep-sea sediments: high-resolution records of flux and dissolution of carbonate in the equatorial Atlantic during the last 24000 years. *Paleoceanography* **5**, 761–787.

Gavish E., and Friedman G. (1969) Progressive diagenesis in Quaternary to Later Tertiary carbonate sediments: sequence and time scale. *J. Sediment. Petrol.* **39**, 980–1006.

Graham D. W., Bender M. L., Williams D. F., and Keigwin, L. D., Jr. (1982) Strontium-calcium ratios in Cenozoic planktonic foraminifera. *Geochim. Cosmochim. Acta* **46**, 1281–1292.

Guilderson T. P., Fairbanks R. G., and Rubenstone J. L. (1994) Tropical temperature variations since 20,000 years ago: Modulating interhemispheric climate change. *Science* **263**, 663–665.

Harris W. H. and Matthews R. K. (1968) Subaerial diagenesis of carbonate sediments: Efficiency of the solution-reprecipitation process. *Science* **160**, 77–79.

Hay W. W. and Southam J. R. (1977) Modulation of marine sedimentation by the continental shelves. In The Fate of Fossil Fuel CO_2 in the Ocean. (ed. N. R. Anderson and A. Malahoff), pp. 569–604 Plenum.

Hess J., Bender M. L., and Schilling J.-G. (1986) Evolution of the ratio of strontium-87 to strontium-86 in seawater from Cretaceous to present. *Science* **231**, 979–984.

Hess J., Stott L. D., Bender M. L., Kennet J. P., and Schilling J.-G. (1989) The Oligocene marine microfossil record: Age assessments using strontium isotopes. *Paleoceanography* **4**, 655–679.

Hodell D. A., Mueller P. A., McKenzie J. A., and Mead G. A. (1989) Strontium isotope stratigraphy and geochemistry of the late Neogene ocean. *Earth Planet. Sci. Lett.* **92**, 165–178.

Holland H. D. (1984) *The Chemical Evolution of the Atmosphere and Oceans*. Princeton University Press.

Kleypas J. A. (1997) Modeled estimates of global reef habitat and carbonate production since the last glacial maximum. *Paleoceanography* **12**, 533–545.

Milliman J. D. (1993) Production and accumulation of calcium carbonate in the ocean: Budget of a nonsteady-state. *Global Biogeochem. Cycles* **7**, 927–957.

Milliman J. D. and Droxler A. W. (1996) Neritic and pelagic carbonate sedimentation in the marine environment: ignorance is not bliss. *Geol. Rundsch.***85**, 496–504.

Morrow D. W. and Mayers I. R. (1978) Simulation of limestone diagenesis—a model based on strontium depletion. *Canadian J. Earth Sci.* **15**, 376–396.

Morse J. W. and Bender M. L. (1990) Partition coefficients in calcite: Examination of factors influencing the validity of experimental results and their application to natural systems. *Chem. Geol.* **82**, 265–277.

Mortlock R. A. et al. (1992) River fluxes of dissolved silicon to the ocean were higher during glacials: Ge/Si in diatoms, rivers, and oceans. *Paleoceanography* **7**, 739–767.

Nurnberg D., Buma J., and Hemleben C. (1996) Assessing the reliability of magnesium in foraminiferal calcite as a proxy for water mass temperatures. *Geochim. Cosmochim. Acta* **60**, 803–814.

Opdyke B. N. and Walker J. C. G. (1992) Return of the coral reef hypothesis: Basin to shelf partitioning of $CaCO_3$ and its effect on atmospheric CO_2. *Geology* **20**, 733–736.

Opdyke B. N., Walker L. M., and Huston T. J. (1993) Fluoride content of foraminiferal calcite: Relations to life habitat, oxygen isotope composition, and minor element chemistry. *Geology* **21**, 169–172.

Opdyke B. N. and Wilkinson B. H. (1988) Surface area control of shallow cratonic to deep marine carbonate accumulation. *Paleoceanography* **3**, 685–703.

Palmer M. R. and Edmond J. M. (1989) The strontium isotope budget of the modern ocean. *Earth Planet. Sci. Lett.* **92**, 11–26.

Richter F. M. and Liang Y. (1993) The rate and consequences of strontium diagenesis in deep-sea carbonates. *Earth Planet. Sci. Lett.* **117**, 553–565.

Richter F. M. and Turekian K. K. (1993) Simple models for the geochemical response of the ocean to climatic and tectonic forcing. *Earth Planet. Sci. Lett.* **119**, 121–131.

Roselle P. (1985) Modern cool-water beach sands of southwest England—a discussion. *J. Sediment. Petrol.* **55**, 778–783.

Schlanger S. O. (1988) Strontium storage and release during deposition and diagenesis of marine carbonates related to sea-level variations. In *Physical and Chemical Weathering in Geochemical Cycles* (ed. A. Lerman and M. Meybeck), pp. 323–339. Kluwer.

Shackleton N. J. and Pisias N. G. (1985) Atmospheric carbon dioxide, orbital forcing, and climate. In *The Carbon Cycle and Atmospheric CO_2: Natural Variations Archean to Present* (ed. E. T. Sundquist and W. S. Broecker); *AGU Monograph* **32**, pp.303–317.

Smith S. V., Buddemeier R. W., Redale R. C., and Houck J. E. (1979) Strontium-calcium thermometry in coral skeletons. *Science* **204**, 404–406.

Stoll H. M. and Schrag D. P. (1996) Evidence for glacial control of rapid sea level changes in the Early Cretaceous. *Science* **272**, 1771–1774.

Turekian K. K. (1963) Rates of calcium carbonate deposition by deep-sea organisms, molluscs, and the coral-algae association. *Nature* **197**, 277–278.

Walker J. C. G. and Opdyke B. C. (1995) Influence of variable rates of neritic carbonate deposition on atmospheric carbon dioxide and pelagic sediments. *Paleoceanography* **10**, 415–427.